Experimental Observation of Two Features Unexpected from the Classical Theories of Rubber Elasticity

Kengo Nishi,[1,2,3,*] Kenta Fujii,[4] Ung-il Chung,[1] Mitsuhiro Shibayama,[2] and Takamasa Sakai[1,†]

[1]*Department of Bioengineering, School of Engineering, University of Tokyo, 7-3-1 Hongo, Bunkyo-ku, Tokyo 113-8656, Japan*
[2]*Institute for Solid State Physics, University of Tokyo, 5-1-5 Kashiwanoha, Kashiwa, Chiba 277-8581, Japan*
[3]*Third Institute of Physics-Biophysics, Georg August University, 37077 Goettingen, Germany*
[4]*Graduate School of Sciences and Technology for Innovation, Yamaguchi University,*
2-16-1 Tokiwadai, Ube, Yamaguchi 755-8611, Japan

Although the elastic modulus of a Gaussian chain network is thought to be successfully described by classical theories of rubber elasticity, such as the affine and phantom models, verification experiments are largely lacking owing to difficulties in precisely controlling of the network structure. We prepared well-defined model polymer networks experimentally, and measured the elastic modulus G for a broad range of polymer concentrations and connectivity probabilities, p. In our experiment, we observed two features that were distinct from those predicted by classical theories. First, we observed the critical behavior $G \sim |p - p_c|^{1.95}$ near the sol-gel transition. This scaling law is different from the prediction of classical theories, but can be explained by analogy between the electric conductivity of resistor networks and the elasticity of polymer networks. Here, p_c is the sol-gel transition point. Furthermore, we found that the experimental $G - p$ relations in the region above C^* did not follow the affine or phantom theories. Instead, all the $G/G_0 - p$ curves fell onto a single master curve when G was normalized by the elastic modulus at $p = 1$, G_0. We show that the effective medium approximation for Gaussian chain networks explains this master curve.

Understanding the elasticity of polymer networks, such as rubbers and gels, is crucially important for materials science and biophysics. The elastic modulus, which is one of the most basic properties of rubber elasticity, has been studied for several decades and is thought to be successfully described by the classical theories such as the affine model and the phantom model [1–3]. However, outstanding problems are clearly observed when the classical theories are applied to networks with topological defects or gelation processes.

The first problem is that the classical theories of rubber elasticity fail in describing the critical behavior near the sol-gel transition, as pointed out by de Gennes [4,5]. The elastic modulus G near the critical region is expected to follow a power law: $G \sim |p - p_c|^f$. Here, p and p_c are the fraction of bonds that connect neighbor sites and the percolation threshold, respectively. The classical theories predict $f = 3$ [3,4], whereas de Gennes and Daoud predict $f = 1.9$ and 2.6, respectively [5,6]. The validity of these predictions is still unclear [7] because experimental values of f are very scattered, ranging from 2 to 4 [8–17]. One reason for these scattered experimental values is that the connectivity probability, p, is difficult to quantify experimentally. Therefore, instead of $|p - p_c|$, parameters such as time, $|t - t_c|$, or temperature, $|T - T_c|$, during the gelation process have been used. Here, t_c and T_c are defined as time and temperature, respectively, at the critical point. Though these approximations for $|p - p_c|$ should be valid

very near the critical point, the validity in the range in which previous experiments were conducted is unclear.

The second problem can be seen in the absolute value of G far from the critical region. In this region, the elastic modulus is thought to be described by the affine, phantom, or junction-affine models [1–3,18,19]. These theories are summarized by the following equation:

$$G = [\nu(C_0, p) - h\mu(C_0, p)]k_B T. \qquad (1)$$

Here, C_0, k_B, T, ν, and μ are the initial polymer concentration, Boltzmann's constant, the absolute temperature, and the number densities of elastically effective chains and crosslinks, respectively. Note that ν and μ depend on C_0 and p. The empirical parameter h has a value of 0 for the affine model, 1 for the phantom model, and $0 < h < 1$ for the junction-affine model. This equation is important not only because the network connectivity and parameters can be evaluated from simple stretching measurements, but also because several theories of elasticity and rheological properties can be constructed based on this relation [20–26]. Though Eq. (1) is a fundamental equation for the elasticity of a polymer network, its validity has not been investigated for a broad range of C_0 and p values. Akagi *et al.* conducted verification experiments of Eq. (1) by varying C_0 only around $p = 1$, and showed that the experimental value of the elastic modulus falls somewhere in between the two limits, i.e., the phantom and affine models. However, they did not

conduct experiments for a broad range of C_0 and p values and found no general correlation between G and network defects. Owing to the uncertainty of Eq. (1), in most cases, the affine model and phantom model are used for rubbers and gels empirically.

One of the reasons why these problems remain unsolved is the lack of precise and reliable experiments with precisely controlled network parameters. Therefore, in this Letter, we constructed well-defined model polymer networks, and evaluated G for a broad range of both C_0 and p. From these experiments, we determined the critical exponent f in the critical region. Furthermore, our examination of the affine and phantom models showed that all the $G - p$ curves fell onto a single master curve, which cannot be explained by the classical theories, when we normalized G by the elastic modulus at $p = 1$, G_0.

Here, we used a model polymer network called Tetra-PEG gel [27], which is formed by A-B–type cross-end coupling of two tetra-arm poly(ethylene glycol) (Tetra-PEG) units. Previous neutron scattering, NMR, and tearing studies of Tetra-PEG gels [28–30] confirmed that (i) inhomogeneity of polymer concentration is largely suppressed, (ii) elastically ineffective loops are reduced, and (iii) there are no trapped entanglements because of the well-defined prepolymer architecture. In a previous study [27], Tetra-PEG prepolymers were equipped with N-hydroxysuccinimide (NHS) or amine groups. However, because the NHS groups underwent spontaneous hydrolysis, the amine groups remained unreacted in the system; this makes the connectivity defects. In addition, the connectivity probability p could not be precisely evaluated by IR measurements owing to the presence of the strong absorption of dissociated NHS. Therefore, we newly prepared Tetra-PEG gels using Tetra-PEG prepolymers modified with mutually reactive maleimine (Tetra-PEG-MA) and thiol (Tetra-PEG-SH) (Fig. 1). We evaluated the time dependence of G and p using rheological and UV measurements.

Samples were prepared by mixing buffer solutions of two kinds of four-arm star polymers, i.e., tetra-maleimide-teminated PEG (Tetra-PEG-MA) and tetra-thiol-terminated PEG (Tetra-PEG-SH) (Nippon Oil and Fat Co.). The molecular weights, M_w, of Tetra-PEG-MA and Tetra-PEG-SH were matched at 20 kg/mol. In order to control the reaction rate, the polymers were dissolved in phosphate-citrate buffer and the pH of the buffer was (i) pH 3.8
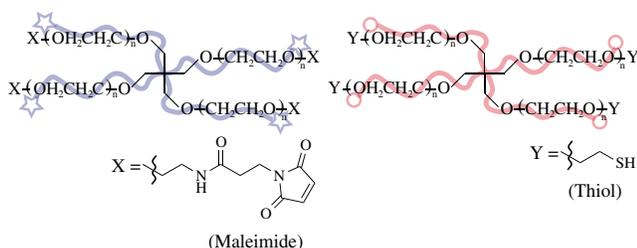
for 10 and 20 mg/mL, (ii) pH 3.4 for 40 mg/mL, and (iii) pH 2.6 for 60–120 mg/mL.

By definition, the connectivity probability p is the connection probability between neighboring sites. Therefore, in this Letter, p is defined as the ratio between reacted maleimide and the total number of arm ends for Tetra-PEG-MA, i.e., $p = \{[\text{MA}](0) - [\text{MA}](t)\}/4[\text{Tetra-PEG-MA}]$. Here, $[\text{MA}](t)$ and $[\text{Tetra-PEG-MA}]$ are the concentration of maleimide at time t and the initial concentration of Tetra-PEG-MA, respectively. To evaluate $[\text{MA}](t)$, we measured the time course of the UV spectrum at 310 nm (JASCO V-630, Nihon-bunko, Japan), as shown in Fig. 2. Here, the UV absorption at 310 nm is assigned to maleimide, as demonstrated in Fig. S1 (see Supplemental Material [31], Sec. I). Some subreactions such as auto-oxidation of thiols and ring-opening of maleimides are well known to occur in solution, and could occur prior to or during hydrogel formation. However, as discussed in Fig. S1, these subreactions are much slower than the main reaction, i.e., the formation of a thioether bond, and therefore we can neglect them. We observed the decrease of maleimide to follow a second-order reaction, as shown in Fig. S2. We estimated $[\text{MA}](t)$ from $A_{310}(t)$, based on the proportional relation between these parameters depicted in Fig. S2 (see Supplemental Material [31], Sec. II). We also measured the time course of the storage elastic modulus (G') and the loss elastic modulus (G'') at a constant frequency (1 Hz) and a strain (2%) by using a rheometer (MCR501, Anton Paar, Austria). The inset of Fig. 2 shows the time courses of G' and G'' during gelation process (40 mg/ml). G' crossed over G'' at around 5490 s, and we assumed that this point corresponds to the sol-gel transition point or the percolation threshold. The connectivity probability at the percolation threshold, p_c, was determined as p at time when G' and G'' crossed over in the rheological measurements. From the UV measurements and rheological measurements, we obtained a relation between G and p, as shown below.

FIG. 1.   Structures for Tetra-PEG prepolymers.
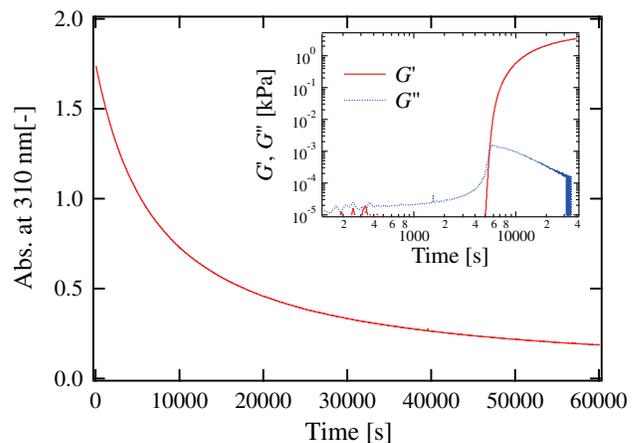
FIG. 2.   Time dependence of the UV absorbance at 310 nm for a polymer concentration of 40 mg/mL. Inset: Time dependence of the storage elastic modulus and the loss elastic modulus.

We plotted p_c as a function of concentration, as shown in the inset of Fig. 3. The dotted line in the inset corresponds to the percolation threshold of a diamond lattice ($p_c = 0.39$). Note that the overlapping concentration, C^*, is around 40 mg/mL according to our previous work [28]. We found that p_c does not depend on polymer concentration and is in close agreement with the percolation threshold of a diamond lattice when the polymer concentration is near or above C^*. These results clearly confirm the ideality of Tetra-PEG gel, the accuracy of the experimental data, and the validity of percolation theory [36]. Note that the percolation threshold for a $z = 4$ Bethe lattice is 0.33, which indicates that this network is better described by percolation theory than a Bethe lattice. Here, z is the coordination number, i.e., the number of arms in a single tetrapolymer. On the other hand, p_c increased with decreasing polymer concentration when the polymer concentration is below 20 mg/mL. This increase of p_c suggests that higher connectivity is necessary for forming an infinite cluster because the space is not fully filled with polymers below 20 mg/mL. G is plotted as a function of $p - p_c$ in Fig. 3. It should be noted that this is the first experiment in which G is plotted as a function of $p - p_c$ near the critical region. According to previous studies [8,37], G' strongly depends on the frequency near the critical point, which is problematic because the plateau values of G' are required for this analysis. However, as demonstrated in Fig. S3, we confirmed that G' does not depend on the frequency when $p - p_c > 0.03$. In addition, we observed a deviation from single power-law behavior at $p - p_c \geq 0.3$ because this range is out of critical region, as shown in a previous study [38]. Thus, we fitted G to a power law for $0.03 \leq p - p_c \leq 0.2$ to evaluate f. The value of the critical exponent f extracted from the figure is 1.95 ± 0.05. This result indicates that the elasticity of gels is analogous to the conductivity of a resistor network, as predicted by de Gennes [5].
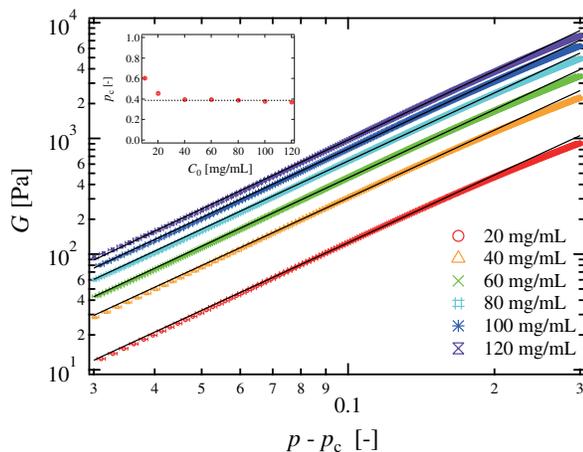
FIG. 3. Critical behavior of the elastic modulus. The solid lines are fits to a power law. Inset: Concentration dependence of the reaction probability at the gelation threshold, p_c. The dotted line corresponds to $p_c = 0.39$, which is the percolation threshold of a diamond lattice.

Next, we focus on the region far from the sol-gel transition point. First, we briefly review previous results for the classical theories of rubber elasticity, such as affine and phantom models. As mentioned above, it is well established that the elastic modulus falls somewhere in between the two limits, i.e., phantom and affine models, as indicated by Eq. (1) [1–3,18,19]. For example, Akagi et al. showed that phantom model is valid around C^* and around $p = 1$, whereas experimental elastic modulus values deviate from phantom model and approach affine model as the polymer concentration increases. In addition, in the previous study, the p dependence of G was only examined in the region around C^* and the phantom model was found to reproduce the experimental results well [39]. However, to the best of our knowledge, the p dependence of G in the region well above C^* is poorly understood. Here, the p dependence of G from 40 to 100 mg/mL and 120 mg/mL is plotted in Figs. S4 and 4(a), respectively. In order to plot the theoretical predictions for affine model and phantom models, we estimated ν and μ by using treelike theory (see Supplemental Material [31], Sec. IV). Note that 40 mg/mL is the C^* value in this Letter as determined in the previous study [28]. As shown in Fig. S4(a) [31], the p dependence of G around C^* is close to the theoretical prediction of the phantom model, as discussed in a previous study [39]. However, as the concentration increases, the experimental $G - p$ relations gradually deviate from the prediction of the phantom model. Here, we defined G_0 as G at $p = 1$ and evaluated G_0 values by a fitting to a linear function for $p > 0.8$ and extrapolating to $p = 1$. The extrapolated values (G_0) are plotted in the inset of Fig. 4(a) together with the predictions of affine and phantom models. As shown in the inset of Fig. 4(a), the elastic modulus around C^* coincides with the prediction of the phantom model, whereas G_0 values deviate from the phantom model and approach the affine model as the concentration increases. Note that these data are highly reproducible, as shown in Fig. S5 [31]. This deviation from the phantom model does not originate from trapped entanglements because the tearing test proved that Tetra-PEG gels have no trapped entanglements [28]. These results agree with the previous observation that the elastic modulus falls somewhere between the two limits, i.e., phantom and affine models [18,19,28]. However, the classical theories cannot predict where in this range the elastic modulus falls. To explore this point, we normalized G by G_0. As shown in Fig. 4(b), all the $G/G_0 - p$ curves fall onto a single master curve. This master curve cannot be explained by the classical theories of rubber elasticity, as shown by the theoretical predictions of $G/G_0 - p$ for the affine model and phantom model plotted in Fig. S6(a) [31], which do not overlap each other.

To understand this master curve, we examined the effective medium approximation. EMA was first developed to describe the conductivity of bond-disordered conductance networks [40] and was subsequently extended to describe diffusivity in porous media [41] and the elasticity
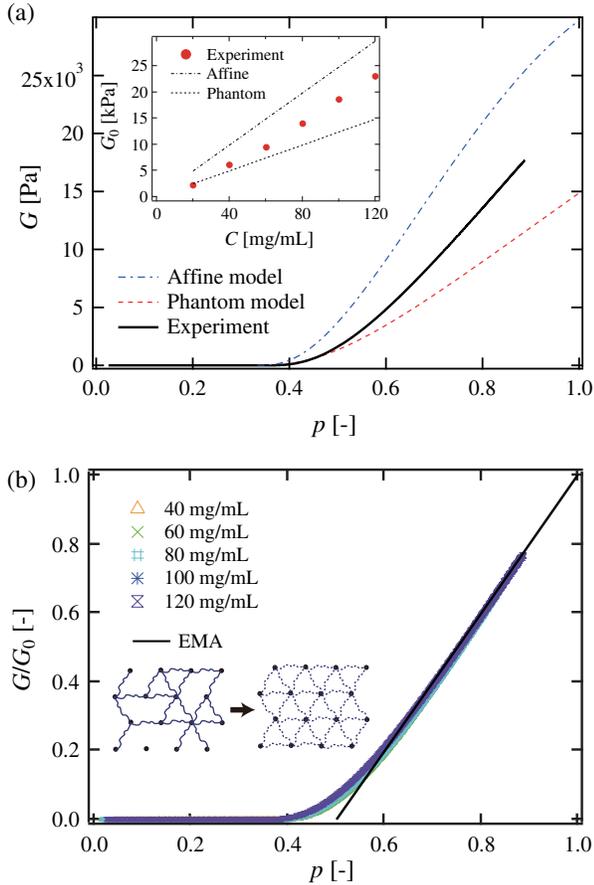
FIG. 4. (a) Experimental $G - p$ plot and theoretical predictions for affine model and phantom models (120 mg/mL). Inset: Concentration dependence of the elastic modulus at $p = 1$, as evaluated from the fitting result. The theoretical predictions of the affine and phantom network model are also shown. (b) p dependence of the reduced elastic modulus at various C_0 values. The solid line corresponds to the theoretical prediction from the effective medium approximation (EMA). Inset: Schematic illustration of the EMA. The network on the left represents the original system in which neighboring sites are randomly connected with chains of elastic constant g_0. The network on the right represents the EMA with a nondisordered structure in which all neighboring sites are connected with chains of elastic constant g_m.

of Hookean spring networks [42]. Recently, significant progress in the EMA has allowed its application to nonlinear elasticity and the dynamical rheology of networks of intracellar biopolymer [43–47]. In a previous study [39], we generalized this EMA theory to the rubber elasticity of Gaussian chain networks. In the EMA theory, we assume that (i) a chain connecting node i to j has potential $U_{ij} = g_0 l_{ij}^2/2$ and (ii) the position of crosslinks can be determined to achieve the force balance. Here, g_0 and l_{ij} are the elastic constant of a single chain and the distance between node i and j, respectively. One should note the following two points. First, the potential in this study is different from that of a Hookean spring network, i.e., $U_{ij} = g_0(l_{ij} - l_0)^2/2$,

where l_0 is the natural length of a Hookean spring. Therefore, our system ($l_0 = 0$) belongs to a different universality class from Hookean spring networks ($l_0 \neq 0$) [48,49], but the same class as the electric conductivity problem. Second, situation (ii) corresponds to the Kirchoff law for the electric conductivity of resistor networks. The main assumption in the EMA is that the bond-disordered network has the same mechanical properties as a nondisordered network with the renormalized elastic constant g_m, as depicted in Fig. 4(b). This value is determined by requiring that the strain fluctuations of nodes in the disordered network from nondisorder network should have a zero average. From this assumption, the ratio of the elastic modulus at p, G, to that at $p = 1$, G_0, should be equal to

$$G/G_0 = (p - 2/z)/(1 - 2/z). \qquad (2)$$

This approximation is valid far above the percolation threshold because the strain fluctuation in the disordered network from nondisordered network becomes quite large near the percolation threshold and the mean-field approximation is broken down as discussed in the previous studies [39,50,51]. As a result, EMA predicts $G \sim |p - p_c|^1$ near the percolation threshold, which is different from our experimental results. Therefore, in this section, we focus on the region far above the percolation threshold as mentioned above. As shown in Fig. 4(b), the prediction of the EMA reproduces the master curve of the $G/G_0 - p$ relation well. This excellent agreement strongly indicates the validity of the EMA framework and the strong correlation among many kinds of networks such as polymer networks, Hookean spring networks, conductance networks, and porous media.

One should note the relation between the classical theories and the EMA. Importantly, when we focus on the p dependence of normalized G, the phantom model coincides with the EMA, whereas the affine does not. To visualize this point, the theoretical predictions of $G/G_0 - p$ for the phantom model and affine model are plotted with that of EMA in Figs. S6(b) and S6(c) [31]. When we focus on C^* concentration, for which the phantom model should be applicable, there is no observable difference between the EMA and the phantom model although the EMA is not based on the classical theories of rubber elasticity. This point was one of the main findings in the previous study based on experiments looking only on C^* concentration and accompanying simulations [39]. On the other hand, when we focus on the $C_0 > C^*$ region, where the affine model should be applicable, a difference between the EMA and the affine model for $p > 0.6$ is observed, as shown in Fig. S6(c), and we can distinguish which theories are valid. This feature has not been pointed out or proved previously owing to the lack of experiments for a broad range of C_0 and p.

Finally, we examined generalization of the present results to more disordered materials. In order to generalize the present results, it is necessary to rewrite equations by using ν or μ instead of p because ν or μ are experimentally

accessible in disordered materials. According to our results, the EMA states that G should always be proportional to $p - 2/z$, ($G \propto p - 2/z$). Moreover, the theoretical prediction of $G/G_0 - p$ for the phantom model and the EMA coincide, as depicted in Fig. S6(b) [31]. Because the $\nu - \mu$ term contributes to the p dependence of G in the phantom model, the above coincidence implies that $\nu - \mu$ is proportional to $p - 2/z$ (i.e., $\nu - \mu \propto p - 2/z$). Therefore, G should be proportional to $\nu - \mu$ (i.e., $G \propto \nu - \mu$). This expression indicates that elastically effective loops play an important role because $\nu - \mu$ corresponds to the number of elastically effective loops [3]. To summarize our Letter, G can be described as

$$G = (\nu - \mu)g_1. \tag{3}$$

Here, g_1 is a proportionally constant. Note that this g_1 value varies with the initial polymer concentration, C_0, which is different from the phantom model, where $g_1 = k_B T$. This functional form shown by Eq. (3) should be useful and applicable for materials that are more disordered than the Tetra-PEG system.

---

[*]kengo.nishi@phys.uni-goettingen.de
[†]sakai@tetrapod.t.u-tokyo.ac.jp

[1] P. J. Flory, *Principles of Polymer Chemistry* (Cornell University Press, Ithaca, 1953).
[2] H. M. James and E. Guth, J. Chem. Phys. **21**, 1039 (1953).
[3] M. Rubinstein and R. H. Colby, *Polymer Physics* (Oxford University Press, New York, 2003).
[4] P. G. de Gennes, *Scaling Concepts in Polymer Physics* (Cornell University Press, Ithaca, 1993).
[5] P. G. de Gennes, J. Phys. Lett. **37**, L1 (1976).
[6] M. Daoud and A. Coniglio, J. Phys. A **14**, L301 (1981).
[7] X. Xing, S. Mukhopadhyay, and P. M. Goldbart, Phys. Rev. Lett. **93**, 225701 (2004).
[8] M. Tokita and K. Hikichi, Phys. Rev. A **35**, 4329 (1987).
[9] M. A. V. Axelos and M. Kolb, Phys. Rev. Lett. **64**, 1457 (1990).
[10] F. Devreux, J. P. Boilot, F. Chaput, L. Malier, and M. A. V. Axelos, Phys. Rev. E **47**, 2689 (1993).
[11] G. C. Fadda, D. Lairez, and J. Pelta, Phys. Rev. E **63**, 061405 (2001).
[12] M. Adam, M. Delsanti, D. Durand, G. Hild, and J. Munch, Pure Appl. Chem. **53**, 1489 (1981).
[13] M. Adam, M. Delsanti, and D. Durand, Macromolecules **18**, 2285 (1985).
[14] J. E. Martin, D. Adolf, and J. P. Wilcoxon, Phys. Rev. Lett. **61**, 2620 (1988).
[15] R. H. Colby, J. R. Gillmor, and M. Rubinstein, Phys. Rev. E **48**, 3712 (1993).
[16] C. P. Lusignan, T. H. Mourey, J. C. Wilson, and R. H. Colby, Phys. Rev. E **52**, 6271 (1995).
[17] C. P. Lusignan, T. H. Mourey, J. C. Wilson, and R. H. Colby, Phys. Rev. E **60**, 5657 (1999).
[18] P. J. Flory, J. Chem. Phys. **66**, 5720 (1977).
[19] P. J. Flory, Polymer **20**, 1317 (1979).
[20] H. Zhou, J. Woo, A. M. Cok, M. Wang, B. D. Olsen, and J. A. Johnson, Proc. Natl. Acad. Sci. U.S.A. **109**, 19119 (2012).
[21] H. Zhou, E. M. Schoen, M. Wang, M. J. Glassman, J. Liu, M. Zhong, D. D. Diaz, B. D. Olsen, and J. A. Johnson, J. Am. Chem. Soc. **136**, 9464 (2014).
[22] R. Wang, A. Alexander-Katz, J. A. Johnson, and B. D. Olsen, Phys. Rev. Lett. **116**, 188302 (2016).
[23] M. Zhong, R. Wang, K. Kawamoto, J. A. Johnson, and B. D. Olsen, Science **353**, 1264 (2016).
[24] Y. Gu, K. Kawamoto, M. Zhong, M. Chen, M. J. A. Hore, A. M. Jordan, L. T. J. Korley, B. D. Olsen, and J. A. Johnson, Proc. Natl. Acad. Sci. U.S.A. **114**, 4875 (2017).
[25] R. Long, K. Mayumi, C. Creton, T. Narita, and C. Y. Hui, Macromolecules **47**, 7243 (2014).
[26] E. B. Stukalin, L. H. Cai, N. A. Kumar, L. Leibler, and M. Rubinstein, Macromolecules **46**, 7525 (2013).
[27] T. Sakai, T. Matsunaga, Y. Yamamoto, C. Ito, R. Yoshida, S. Suzuki, N. Sasaki, M. Shibayama, and U. Chung, Macromolecules **41**, 5379 (2008).
[28] Y. Akagi, J. P. Gong, U. Chung, and T. Sakai, Macromolecules **46**, 1035 (2013).
[29] T. Matsunaga, T. Sakai, Y. Akagi, U. Chung, and M. Shibayama, Macromolecules **42**, 1344 (2009).
[30] T. Matsunaga, T. Sakai, Y. Akagi, U. Chung, and M. Shibayama, Macromolecules **42**, 6245 (2009).
[31] See Supplemental Material at http://link.aps.org/supplemental/10.1103/PhysRevLett.119.267801 for auxiliary methods section and data, which includes Refs. [32–35].
[32] A. D. Baldwin and K. L. Kiick, Polym. Chem. **4**, 133 (2013).
[33] L. D. Freedman and A. H. Corwin, J. Biol. Chem. **181**, 601 (1949).
[34] A. D. Baldwin and K. L. Kiick, Bioconjugate Chemistry **22**, 1946 (2011).
[35] D. R. Miller and C. W. Macosko, Macromolecules **9**, 206 (1976).
[36] D. Staufer, *Percolation Theory for Mathematicians* (Birkhauser, Boston, 1982).
[37] H. H. Winter and F. Chambon, J. Rheol. **30**, 367 (1986).
[38] O. Farago and Y. Kantor, Europhys. Lett. **52**, 413 (2000).
[39] K. Nishi, H. Noguchi, T. Sakai, and M. Shibayama, J. Chem. Phys. **143**, 184905 (2015).
[40] S. Kirkpatrick, Rev. Mod. Phys. **45**, 574 (1973).
[41] M. Sahimi, Rev. Mod. Phys. **65**, 1393 (1993).
[42] S. Feng, M. F. Thorpe, and E. Garboczi, Phys. Rev. B **31**, 276 (1985).
[43] M. Das, F. C. MacKintosh, and A. J. Levine, Phys. Rev. Lett. **99**, 038101 (2007).
[44] C. P. Broedersz, C. Storm, and F. C. MacKintosh, Phys. Rev. E **79**, 061914 (2009).

[45] M. Sheinman, C. P. Broedersz, and F. C. MacKintosh, Phys. Rev. E **85,** 021801 (2012).

[46] M. G. Yucht, M. Sheinman, and C. P. Broedersz, Soft Matter **9,** 7000 (2013).

[47] C. P. Broedersz and F. C. MacKintosh, Rev. Mod. Phys. **86,** 995 (2014).

[48] M. Dennison, M. Sheinman, C. Storm, and F. C. MacKintosh, Phys. Rev. Lett. **111,** 095503 (2013).

[49] M. Jaspers, M. Dennison, M. F. J. Mabesoone, F. C. MacKintosh, A. E. Rowan, and P. H. J. Kouwer, Nat. Commun. **5,** 5808 (2014).

[50] M. Sahimi, B. D. Hughes, L. E. Scriven, and H. T. Davis, Phys. Rev. B **28,** 307 (1983).

[51] C. P. Broedersz, X. Mao, T. M. Lubensky, and F. C. MacKintosh, Nat. Phys. **7,** 983 (2011).